Published in final edited form as:
JACC Cardiovasc Imaging. 2010 January ; 3(1): 32–40. doi:10.1016/j.jcmg.2009.10.009.

Segmental heterogeneity of vasa vasorum neovascularization in human coronary atherosclerosis and role of intraplaque hemorrhage in plaque calcification

Mario Gössl, MD[1], **Daniele Versari, MD**[1], **Heike A. Hildebrandt**[1], **Thomas Bajanowski, MD**[2], **Giuseppe Sangiorgi, MD**[3], **Raimund Erbel, MD, FACC**[4], **Erik L. Ritman, MD, PhD**[5], **Lilach O Lerman, MD, PhD**[6], and **Amir Lerman, MD, FACC**[1]

[1]The Division of Cardiovascular Diseases, Mayo Clinic College of Medicine, Rochester, MN, USA

[2]Institute of Forensic Medicine, University Duisburg-Essen, Hufelandstr. 55, 45122 Essen, Germany

[3]Mediolanum Cardio Research, 20145 Milan, Italy

[4]Clinic of Cardiology, West-German Heart-Center, University Duisburg-Essen, Hufelandstraβe 55, 45122 Essen, Germany

[5]Department of Physiology and Biomedical Engineering, Mayo Clinic College of Medicine, Rochester, MN, USA

[6]Division of Nephrology and Hypertension, Mayo Clinic College of Medicine, Rochester, MN, USA

Abstract

Objectives—To investigate the role of coronary vasa vasorum (VV) neovascularization in the progression and complications of human coronary atherosclerotic plaques.

Background—Accumulating evidence supports an important role of VV neovascularization in atherogenesis and lesion location determination in coronary artery disease. VV neovascularization can lead to intraplaque hemorrhage, which has been identified as a promoter of plaque progression and complications like plaque rupture. We hypothesized that distinctive patterns of VV neovascularization and associated plaque complications can be found in different stages of human coronary atherosclerosis.

Methods—Hearts from 15 patients (age 52±5, mean±SEM) were obtained at autopsy, perfused with Microfil™ and subsequently scanned with micro-computed tomography (micro-CT). Two-cm-segments (n=50) were histologically classified as either normal (n=12), nonstenotic plaque (<50% stenosis, n=18), or calcified (n=10) or non-calcified (n=10) stenotic plaque. Micro-CT images were analyzed for VV density (#/mm^2), VV vascular area fraction (mm^2/mm^2) and VV endothelial surface fraction (mm^2/mm^3). Histological sections were stained for Mallory's (iron), von Kossa (calcium) and glycophorin-A (erythrocyte fragments) as well as endothelial nitric oxide

Address of Correspondence: Amir Lerman, M.D., Division of Cardiovascular Diseases, Mayo Clinic Rochester, 200 First Street S.W., Rochester, MN, 55905, USA, Phone: (507)-255-4152, Fax: (507)-255-2550, lerman.amir@mayo.edu.

The authors have no relevant conflict of interest or financial disclosure to make.

synthase (eNOS), vascular endothelial growth factor (VEGF) and tumor necrosis factor-alpha (TNF-α).

Results—VV density was higher in segments with non-stenotic and non-calcified stenotic plaques as compared to normals (3.36±0.45, 3.72±1.03 vs. 1.16±0.21, P<0.01). In calcified stenotic plaques VV spatial density was lowest (0.95±0.21, P<0.05 vs. non-stenotic and non-calcified stenotic plaque). The amount of iron and glycophorin A was significantly higher in non-stenotic and stenotic plaques as compared to normals, and correlated with VV density (Kendall-Tau correlation-coefficient 0.65 and 0.58 respectively, P<0.01). Moreover, relatively high amounts of iron and glycophorin A were found in calcified plaques. Further immunohistochemical characterization of VV revealed positive staining for eNOS and TNF-α but not VEGF.

Conclusion—Our results support a possible role of VV neovascularization, VV rupture and intraplaque hemorrhage in the progression and complications of human coronary atherosclerosis.

Keywords

vasa vasorum; human coronary atherosclerosis; micro-CT; calcification; intraplaque hemorrhage

Introduction

Atherosclerosis is a progressive, inflammatory disease of the vascular wall that begins in an early age as fatty streaks and progresses into raised lesions and mature atheromas in adulthood, often containing calcium hydroxyapatite deposits (1). A high correlation between the histological extent of the atherosclerotic plaque and its calcium deposition has been shown in the coronary vessels for all ages and both sexes making the calcification a surrogate measure of coronary atherosclerosis (2). Traditionally, the outer wall, which includes the adventitial layer and the vasa vasorum (VV), has been considered to play a passive role in atherogenesis. In contrast to this view, previous reports suggest that the adventitial layer may play a significant role in maintaining vessel integrity, and may contribute to the initiation and progression of the atherosclerotic process as well as of the remodeling process (3). Indeed, experimental studies demonstrated that manipulation of the adventitia, and more specifically of the vasa vasorum, could lead to changes in the intimal layer, resembling the atherosclerotic process (4). Using micro computerized tomography (micro-CT) technology in large animal models, we have demonstrated that early atherosclerosis is associated with neovascularization of the vasa vasorum (5). Among other mechanisms, VV may contribute to progression of atherosclerosis by virtue of mediating, localizing and promoting the influx of lipids and infiltrates of inflammatory cells, which are characteristic of unstable plaques (6,7). Moreover, fragility of newly formed vasa vasorum and tendency to leak or break may mediate intra-plaque hemorrhage, which is a major event occurring frequently during the development of the atherosclerotic lesion (8) that can progress acutely to plaque rupture, eventually resulting in a thromboembolic event or acute occlusion of the vessel (9,10).

Thus, it may be speculated that VV neovascularization has a role in the initiation and progression stages of atherosclerosis, by promoting cell proliferation, migration, and matrix production in the plaque. The current study was designed to test the hypothesis that segmental VV neovascularization and its complications of vasa vasorum rupture and intraplaque hemorrhage correlate with the development and progression of human coronary atherosclerotic plaques.

Methods

Specimens

The study protocol was reviewed and approved by the Mayo Foundation Institutional Review Board. Fifty coronary arterial segments (from 20 coronary arteries: 10 LADs, 5 RCAs, 5 LCXs) were obtained at autopsy from 15 patients. Patients' clinical data were obtained by reviewing the clinical files and documented by codes to avoid any identifying details. Artery segments were histologically classified as normal when no atherosclerotic plaque was present (n=12). Segments with mild, non lumen-compromising plaque (<50% lumen diameter stenosis) were classified as non-stenotic plaque (n=18). If lumen-compromising atherosclerotic plaque was present on histology (>50% lumen diameter stenosis) the segments were either classified as non-calcified stenotic (n=10, <50% plaque area calcification) or calcified stenotic plaque (>50% lumen diameter stenosis and >50% plaque area calcification, n=10). Calcification was defined as plaque calcification.

Micro-Computed Tomography (Micro-CT) Analysis

Specimen preparation and imaging—During autopsy the hearts were harvested with specific care for the tissue surrounding the arteries in order to avoid damage to the adventitia. The coronary arteries were injected with Microfil™ (Flow Tech, Inc. Carver, MA) and prepared for micro-CT scanning as described in detail previously (11).

Analysis—Data analysis was performed using Analyze® software (Biomedical Imaging Resource, Rochester, MN). In each segment, 35 to 40 cross-sections at 400 μm intervals were chosen for region of interest analysis and averaged (12). In each micro-CT cross-section, the vessel wall area (defined by the outer border of the adventitia) was determined as described in detail before (5,11). Vasa vasorum parameters were determined as described in detail before (13). A connectivity tool, included in the Analyze® software, was applied on the 3D images of the arterial segments. As shown in Figure 1, this tool enables the identification of the vascular "tree" of each VV and tracking of its origin. That way, internal VV (originating directly from the main lumen) can be differentiated from external VV (originating from a major coronary branch) (11). The subsequent 2D image analysis ensures including only those VV that are actually perfused, i.e. connected to the systemic circulation, and excluding vessels that are in close proximity to the adventitia but are actually not VV.

Histology

After embedding in paraffin, cross-sections of the arteries were mounted on slides and stained with H&E. Parallel histology cross sections were used to confirm the accuracy of adventitial outer border tracing and VV identification in the micro-CT images as described in detail in (11).

Von Kossa Calcium Staining—Sections were deparaffinized, hydrated to distilled water and placed in 6% sliver nitrate for 30 minutes in an incubator. Afterwards, the sections were rinsed in distilled water and incubated in 5% sodium thiosulfate for 5 minutes. The sections were washed in running tap water for 5 minutes and counterstained in 0.1% nuclear fast red for 3 minutes. After rinsing in distilled water, the sections were mounted and visualized under microscope (Figure 2).

Glycophorin A Staining—Erythrocytes fragments within calcified and non-calcified plaques were identified using antibodies against glycophorin A (CD235a, 1:100; DakoCytomation) on deparaffinized histology sections (Figure 3). Normal human bone marrow sections were used for positive controls.

Mallory's Iron Staining—After deparaffinizing and hydrating in water, the sections were stained in potassium ferrocyanide/hydrochloric acid solution (50 ml 5% potassium ferrocyanide, 50 ml 5% hydrochloric acid) for 10 minutes. The sections were rinsed in distilled water, stained in nuclear fast red for 5 minutes and washed in running water for 2 minutes. Finally the sections were mounted and visualized under microscope.

VEGF, TNF-α and eNOS Staining—The slides were cut at 4 microns. Antigen retrieval was performed using a Black and Decker rice steamer and Dako Antigen Retrieval Solution. The slides were then blocked with 5% Hydrogen Peroxide for 15 minutes. Factor VIII antibody (1:50) was left on for 30 minutes. The Dako LSAB2 kit was used for the secondary and tertiary steps. Dako DAB chromogen was used. Following this, the slides were placed in the appropriate antibody (eNOS, predilute; VEGF, 1:250, TNF-α, 1:50) for 60 minutes. The Dako LSAB2-AP kit was used for the second half of staining followed by the Permanent Red chromogen.

Glycophorin A and Iron scoring—The percentage of vessel wall/plaque area showing glycophorin A and iron deposits was graded semi quantitatively by two independent observers using a scale from 0 to 4, with higher scores indicating higher percentages (1 - <25%, 2 - >25 but <50%, 3 - >50 but <75%, 4 - >75%).

Statistical Analysis

Continuous data are expressed as mean ± standard error of the mean. One-way ANOVA, followed by a Tukey-Kramer post hoc test with correction for multiple comparisons, was used to identify the statistical differences among groups. Individual group comparisons were performed by an unpaired Student *t*-test. Statistical significance was accepted for a value of $P<0.05$.

Results

Patients and arterial segments characteristics

Clinical data are summarized in Table 1. The cause of death was trauma (n=8), sepsis (n=6) and suicide (n=1).

Micro-CT data

VV spatial density was significantly higher in coronary segments with non-stenotic and non-calcified stenotic plaques as compared to normal and calcified stenotic plaque segments (Table 2). Calcified plaque segments actually had a spatial VV density similar to normal segments. These data conceivably also translated into significantly higher VV vascular area fractions and VV endothelial surface fractions in non-stenotic and non-calcified stenotic plaques compared to normal and calcified stenotic plaque segments. Adding up the endothelial surface area of all VV within the vessel wall showed that as much as 45% and 67% of the calculated main luminal endothelial surface area is available through the VV in the vessel wall of non-stenotic and non-calcified stenotic plaques (significantly more than in normal segments (17%)). Although VV density and fractions were not different in calcified stenotic plaque segments compared to normals, with 32% there was still significantly more endothelial exchange surface available through the VV in the calcified than in normal vessel wall (Table 2).

There was a significantly higher ratio of external/internal VV in non-calcified stenotic plaque segments compared to all other segments. The ratio already tended to be higher in non-stenotic plaques compared to normal segments (Figure 4).

Histology

Using van Kossa (calcium deposits), Mallory's (iron, hemosiderin) and glycophorin-A staining (erythrocyte fragments) we were able to identify intraplaque hemorrhage likely through vasa vasorum rupture in non-calcified and calcified plaques (Figure 2 and Figure 3). Interestingly, plaque calcification was associated with iron and glycophorin A staining suggesting that recurrent intraplaque hemorrhage is associated with plaque calcification (Figure 2). VV density correlated negatively with the area of calcification ($r=0.42$, $p<0.001$, Figure 4).

Further characterization of VV revealed staining for the endothelial nitric oxide synthase (eNOS), the inflammatory marker tumor necrosis factor-alpha (TNF-α) but not the vascular endothelial growth factor (VEGF, Figure 5). There was no significant difference in the above-described stains between the different plaque types, except for a higher tendency for positive TNF-α staining of VV within diseased coronary artery segments.

Glycophorin A and Iron scores—As shown in Figure 3 and Table 2 the non-stenotic and non-calcified stenotic plaque segments had significantly higher scores of glycophorin A and iron staining than normal and calcified stenotic plaque segments. The Kendall-Tau-*b* rank correlation coefficient for VV density and iron score were 0.65 ($P<0.01$) and 0.58 for VV density and glycophorin A score ($P<0.01$), respectively.

Discussion

The current study demonstrates a significant difference in the pattern of vasa vasorum distribution in human coronary arteries in different stages of atherosclerosis. Vasa vasorum spatial density was higher in artery segments with non-stenotic plaques and further increased in segments with non-calcified stenotic plaque. Overall, vasa vasorum neovascularization in non-stenotic and stenotic plaques was strongly correlated with the histological markers of intraplaque hemorrhage. Nevertheless, once the plaques showed significant calcification, VV spatial density significantly decreased to levels not different from normal coronary segments. Indeed, there was a negative correlation between VV density and the area of calcification within calcified coronary artery sections in micro-CT. However, compared to normal segments calcified plaque segments had higher glycophorin A and iron scores indicating past intraplaque hemorrhages. Hence, the current study further supports the association between adventitial vasa vasorum neovascularization and the progression and complication phases of the atherosclerosis process.

The current study is in accord with previous autopsy studies and supports the notion of a role of intraplaque hemorrhage (iron and glycophorin A deposits), by virtue of VV rupture or an injury to the endothelial lining of the main coronary lumen, in the mechanism of plaque calcification. The mechanism of this process may be speculated upon: the immature vasa vasorum vasculature tends to leak and together with rupture of fragile VV neovasculature leading to intraplaque hemorrhage this may support the development of calcified plaque segments and may be a natural attempt to stabilize the plaque after subclinical intraplaque hemorrhage that did not lead to a plaque rupture and major coronary occlusion and sudden cardiac death.

The atherosclerotic process has a heterogeneous distribution on the surface of the vascular tree, as observed in autopsies as well as in coronary angiography and intravascular ultrasound studies (14). The mechanism of this non-uniform expression can be partially explained by different shear stress forces in regions like bifurcations and curves (15). However, hemodynamic mechanisms may not completely explain the heterogeneity of plaque distribution within arterial segments and even at the same cross section. Hence, it has

become important to identify co-factors for plaque initiation and progression as well as complication in order to assess the plaque burden accurately and modify the natural history of the disease. Utilizing micro-CT, we have previously demonstrated, in the human and porcine circulation, the heterogeneity of adventitial vasa vasorum density among different vascular beds in relation to their known susceptibility to develop atherosclerosis (16,17). In addition, we found that VV spatial density is increased in hypercholesterolemic porcine coronary arteries compared with normal pigs, suggesting a significant role for the adventitial vasa vasorum in the early atherosclerotic remodeling process prior to vasofunctional alterations and plaque formation (18).

Vessels with mild atherosclerosis exhibit proliferation of VV in the adventitia that results in increased VV count and density. Based on our 3D analysis VV neovascularization is pronounced at the level of external VV, the ratio of external VV to internal VV never becomes <1 during the atherosclerotic process although it has been demonstrated that growth of internal VV is stimulated by neointima formation, likely secondary to higher oxygen demand of the tissue (19). This remodeling of the adventitia is further increased in segments with evident plaque. Although VV neovascularization may serve as a compensatory mechanism to counteract vessel wall ischemia, the extensive VV network may function as a conduit for further entry of macrophages and inflammatory factors that may potentially promote the progression of inflammation and plaque formation. Indeed, inhibition of angiogenesis has been shown to reduce macrophages in the plaque and around the vasa vasorum (20). Further characterization of VV in our studies using immunohistochemistry showed expression of eNOS in all plaque types and expression of TNF-α especially in diseased segments. We did not observe expression of VEGF, which may have been affected by the age and processing of the specimen.

The neovascularization process which accompanies the evolution of the atherosclerotic process, leads to the formation of many new vessels and therefore to an increased probability of intraplaque hemorrhage. This process is also enhanced by the tortuosity and frailty of the new-formed microvessels. Intraplaque hemorrhage is associated with increase in the size of the necrotic core and lesion instability in coronary plaques (6). However, before the final plaque rupture, the deposition of blood product in the plaque interstitium (21) may be responsible for the further stimulation of the inflammatory process and can be followed by the organization and fibrosclerosis, leading eventually to calcium deposition.

Coronary artery calcification is pathognomonic of atherosclerosis and its extent is related to the plaque burden and not to the degree of obstruction (22). Identification and quantification of arterial calcification is a reliable method of predicting the risk of cardiovascular events, especially when the calcium score is adjusted to age and sex (23). Arterial calcification is known to start in early stages of atherosclerosis and to represent an active process of mineralization and hydroxyapatite crystals deposition (24). Moreover, a recent study demonstrated that microcalcification is associated with plaque vulnerability and positive remodeling (25). However, the mechanism and the source of the calcification process, whether it is part of the damage, e.g. inflammation, or part of the repair process involving osteogenic endothelial progenitor cells (26), is still under investigation.

Study limitations

This autopsy study represents a selected patient cohort; an inherent selection bias cannot be excluded.

Due to the sample preparation process, no molecular mechanistic studies can be performed on the same arterial segment to explore the molecular mechanisms of VV neovascularization and plaque formation. Furthermore, as a correlative study, the results cannot determine

causation; in particular, even if it is likely that calcium deposition followed repeated plaque VV rupture/hemorrhage, it is possible that a primitive fibrosclerotic process, induced by the inflammatory process, may induce deposition of calcium and make the plaque less metabolically active and less in need of nourishment, causing eventually a decrease in VV density. However, it is unlikely that the increased amount of vessels found in the mature, non-calcified plaque can spontaneously regress. Alternatively they could be compressed by surrounding fibrosclerotic tissue, thus becoming invisible for micro-CT, which detects only patent microvessels connected to the circulation. Also, the observed evidence for VV rupture in the form of iron and glycophorin A deposits may have occurred after the process of plaque calcification, the current study design did not allow looking at different time points of plaque progression. In the current study we did not determine iron deposition using micro-CT technology as shown previously in rodent studies (27).

Conclusion

The current study supports a role for coronary VV not only in the initiation of atherosclerosis but throughout the atherosclerotic process, including the progression phase, i.e. plaque growth and remodeling, and complication phase, i.e. intra-plaque hemorrhage and calcification. The strong association of iron and glycophorin A deposits in calcified plaques may indicate that recurrent vasa vasorum rupture and intraplaque hemorrhage promotes plaque calcification. The segmental heterogeneity of VV and early evidence of intraplaque hemorrhage further support the role of the VV in the focal complication of coronary atherosclerosis. In-vivo imaging techniques assessing vasa vasorum neovascularization in atherosclerosis may help to further define plaque vulnerability and guide medical therapy in the future (28).

Abbreviation list

eNOS	endothelial Nitric Oxide Synthase
ESA	Endothelial Surface Area
Micro-CT	Micro-Computed Tomography
TNF-α	Tumor Necrosis Factor-alpha
VV	Vasa Vasorum
VEGF	Vascular Endothelial Growth Factor

Acknowledgments

This work was supported by the National Institutes of Health (R01 HL63911, K-24 HL69840-02, RO1 HL65432 and RO1 EB000305), and the Mayo Clinic College of Medicine. Dr. Amir Lerman is an Established Investigator of the American Heart Association.

References

1. Agatston AS, Janowitz WR, Hildner FJ, Zusmer NR, Viamonte M Jr, Detrano R. Quantification of coronary artery calcium using ultrafast computed tomography. J Am Coll Cardiol 1990;15:827–832. [PubMed: 2407762]
2. Janowitz WR, Agatston AS, Kaplan G, Viamonte M Jr. Differences in prevalence and extent of coronary artery calcium detected by ultrafast computed tomography in asymptomatic men and women. Am J Cardiol 1993;72:247–254. [PubMed: 8342500]
3. Barker SG, Tilling LC, Miller GC, et al. The adventitia and atherogenesis: removal initiates intimal proliferation in the rabbit which regresses on generation of a 'neoadventitia'. Atherosclerosis 1994;105:131–144. [PubMed: 8003089]

4. Nakata Y, Kamiya K. An experimental study on the vascular lesions caused by obstruction of the vaso vasorum. II. Special consideration on the deposition of fat into vascular wall. Jpn Circ J 1970;34:1029–1034. [PubMed: 5537976]
5. Herrmann J, Lerman LO, Rodriguez-Porcel M, et al. Coronary vasa vasorum neovascularization precedes epicardial endothelial dysfunction in experimental hypercholesterolemia. Cardiovasc Res 2001;51:762–766. [PubMed: 11530109]
6. Kolodgie FD, Gold HK, Burke AP, et al. Intraplaque hemorrhage and progression of coronary atheroma. N Engl J Med 2003;349:2316–2325. [PubMed: 14668457]
7. Virmani R, Kolodgie FD, Burke AP, et al. Atherosclerotic plaque progression and vulnerability to rupture: angiogenesis as a source of intraplaque hemorrhage. Arterioscler Thromb Vasc Biol 2005;25:2054–2061. [PubMed: 16037567]
8. Virmani R, Burke AP, Farb A, Kolodgie FD. Pathology of the vulnerable plaque. J Am Coll Cardiol 2006;47:C13–C18. [PubMed: 16631505]
9. Moreno PR, Purushothaman KR, Fuster V, et al. Plaque neovascularization is increased in ruptured atherosclerotic lesions of human aorta: implications for plaque vulnerability. Circulation 2004;110:2032–2038. [PubMed: 15451780]
10. Burke AP, Farb A, Malcom GT, Liang YH, Smialek J, Virmani R. Coronary risk factors and plaque morphology in men with coronary disease who died suddenly. N Engl J Med 1997;336:1276–1282. [PubMed: 9113930]
11. Gossl M, Rosol M, Malyar NM, et al. Functional anatomy and hemodynamic characteristics of vasa vasorum in the walls of porcine coronary arteries. Anat Rec A Discov Mol Cell Evol Biol 2003;272:526–537. [PubMed: 12740947]
12. Gossl M, Versari D, Mannheim D, Ritman EL, Lerman LO, Lerman A. Increased spatial vasa vasorum density in the proximal LAD in hypercholesterolemia-Implications for vulnerable plaque-development. Atherosclerosis. 2006
13. Gossl M, Zamir M, Ritman EL. Vasa vasorum growth in the coronary arteries of newborn pigs. Anat Embryol 2004;208:351–357. [PubMed: 15309629]
14. Balghith MA, Schoenhagen P, Foody JM, et al. Atherosclerotic plaque distribution in the left anterior descending coronary artery as assessed by intravascular ultrasound. Am J Cardiol 2003;91:443–445. [PubMed: 12586261]
15. Stone PH, Coskun AU, Kinlay S, et al. Effect of endothelial shear stress on the progression of coronary artery disease, vascular remodeling, and in-stent restenosis in humans: in vivo 6-month follow-up study. Circulation 2003;108:438–444. [PubMed: 12860915]
16. Galili O, Herrmann J, Woodrum J, Sattler KJ, Lerman LO, Lerman A. Adventitial vasa vasorum heterogeneity among different vascular beds. J Vasc Surg 2004;40:529–535. [PubMed: 15337884]
17. Hildebrandt HA, Gossl M, Mannheim D, et al. Differential distribution of vasa vasorum in different vascular beds in humans. Atherosclerosis 2008;199:47–54. [PubMed: 17959180]
18. Herrmann J, Best PJ, Ritman EL, Holmes DR, Lerman LO, Lerman A. Chronic endothelin receptor antagonism prevents coronary vasa vasorum neovascularization in experimental hypercholesterolemia. J Am Coll Cardiol 2002;39:1555–1561. [PubMed: 11985922]
19. Ohta O, Kusaba A. Development of vasa vasorum in the arterially implanted autovein bypass graft and its anastomosis in the dog. Int Angiol 1997;16:197–203. [PubMed: 9405016]
20. Moulton KS, Vakili K, Zurakowski D, et al. Inhibition of plaque neovascularization reduces macrophage accumulation and progression of advanced atherosclerosis. Proc Natl Acad Sci U S A 2003;100:4736–4741. [PubMed: 12682294]
21. Virmani R, Kolodgie FD, Burke AP, Farb A, Schwartz SM. Lessons from sudden coronary death: a comprehensive morphological classification scheme for atherosclerotic lesions. Arterioscler Thromb Vasc Biol 2000;20:1262–1275. [PubMed: 10807742]
22. Eggen DA, Strong JP, McGill HC Jr. Coronary calcification. Relationship to clinically significant coronary lesions and race, sex, and topographic distribution. Circulation 1965;32:948–955. [PubMed: 5845254]
23. Raggi P. Detection and quantification of cardiovascular calcifications with electron beam tomography to estimate risk in hemodialysis patients. Clin Nephrol 2000;54:325–333. [PubMed: 11076109]

24. Doherty TM, Asotra K, Fitzpatrick LA, et al. Calcification in atherosclerosis: bone biology and chronic inflammation at the arterial crossroads. Proc Natl Acad Sci U S A 2003;100:11201–11206. [PubMed: 14500910]

25. Shimada Y, Yoshiyama M, Kobayashi Y, et al. Positive correlation between coronary arterial remodelling and prodromal angina in acute myocardial infarction. Heart 2004;90:444–445. [PubMed: 15020526]

26. Gossl M, Modder UI, Atkinson EJ, Lerman A, Khosla S. Osteocalcin expression by circulating endothelial progenitor cells in patients with coronary atherosclerosis. J Am Coll Cardiol 2008;52:1314–1325. [PubMed: 18929243]

27. Langheinrich AC, Michniewicz A, Sedding DG, et al. Quantitative X-ray imaging of intraplaque hemorrhage in aortas of apoE(−/ −)/LDL(−/ −) double knockout mice. Invest Radiol 2007;42:263–273. [PubMed: 17414521]

28. Coli S, Magnoni M, Sangiorgi G, et al. Contrast-enhanced ultrasound imaging of intraplaque neovascularization in carotid arteries: correlation with histology and plaque echogenicity. J Am Coll Cardiol 2008;52:223–230. [PubMed: 18617072]

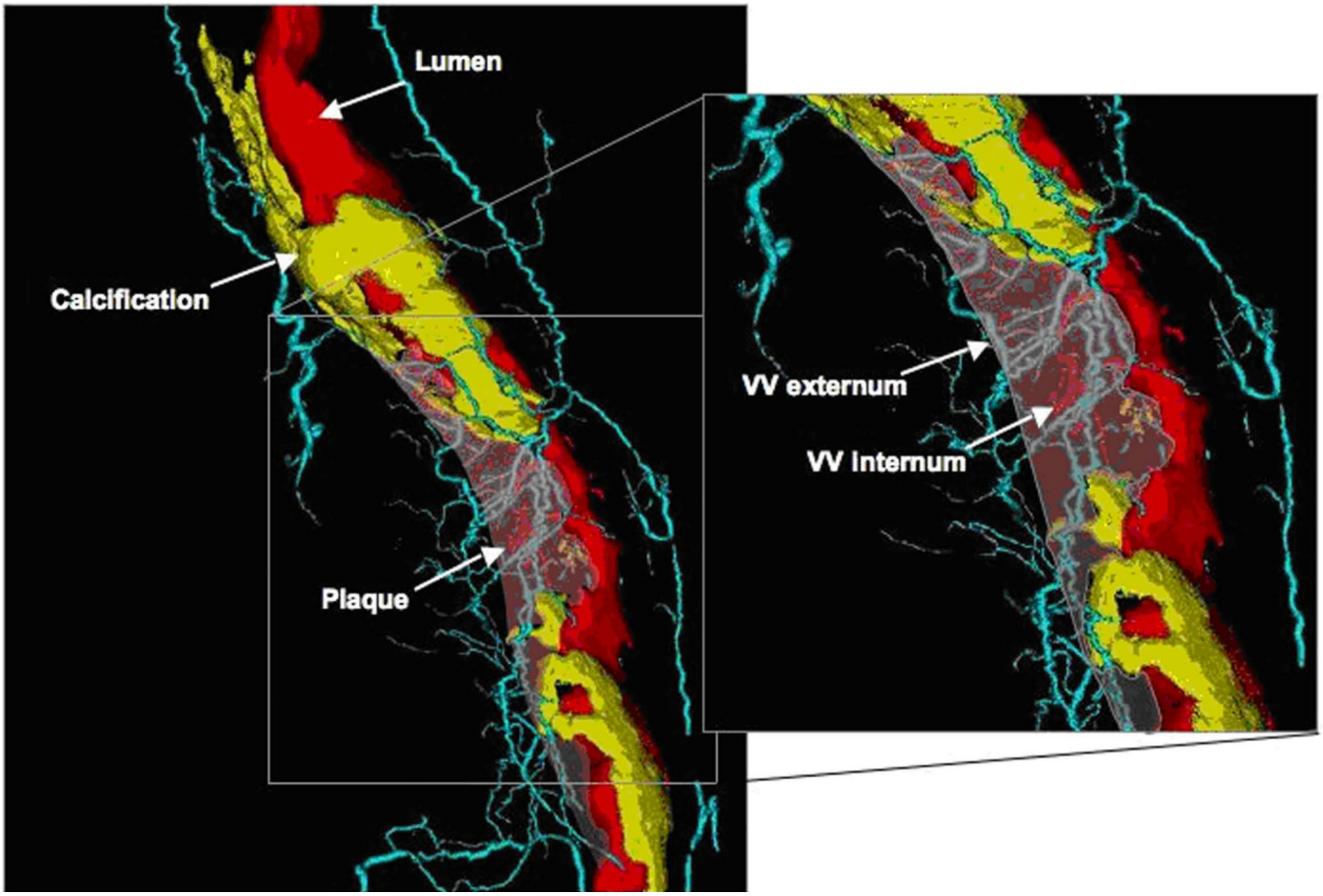

Figure 1. Volume-rendered micro-CT imaging of a coronary plaque and VV

Volume rendered 3D micro-CT image of an RCA showing the main coronary lumen in red, non-calcified and calcified plaque areas are indicated by the arrows (non-calcified plaque is transparent). VV are shown in light blue (VV externa) or red (VV interna, directly originating from the main lumen).

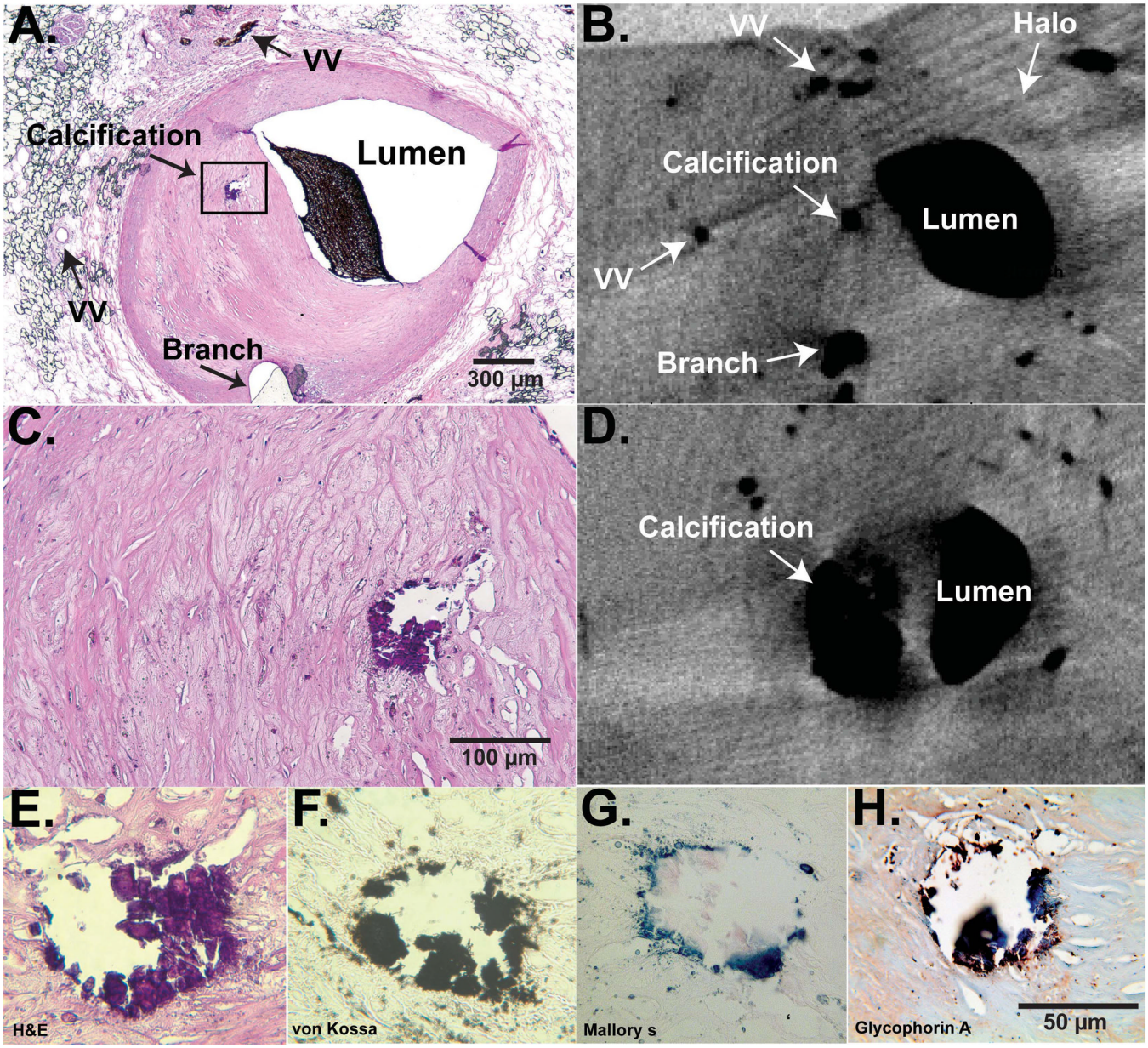

Figure 2. Micro-CT and histology of a calcified stenotic plaque

Panel A: H&E cross-sectional histology slide of an LAD, anatomical landmarks for matching histology with micro-CT are labeled. Panel B: corresponding micro-CT image close to the same level of the histology section. A plaque-calcification is shown as a dark intensity, the luminal intensity represents Microfil. Indicated is also the “halo” which identifies the outer adventitial border. Panel C: magnified view of the plaque in panel A. Panel D: micro-CT cross-section upstream of section in panel B, the calcification is shown in its largest extend. Panels E–H: different stains of the calcified area, H&E, von Kossa for calcium, Mallory’s for iron/hemosiderin, and glycophorin A for erythrocyte fragments. These representative examples demonstrate the close association of calcium and evidence for intraplaque hemorrhage.

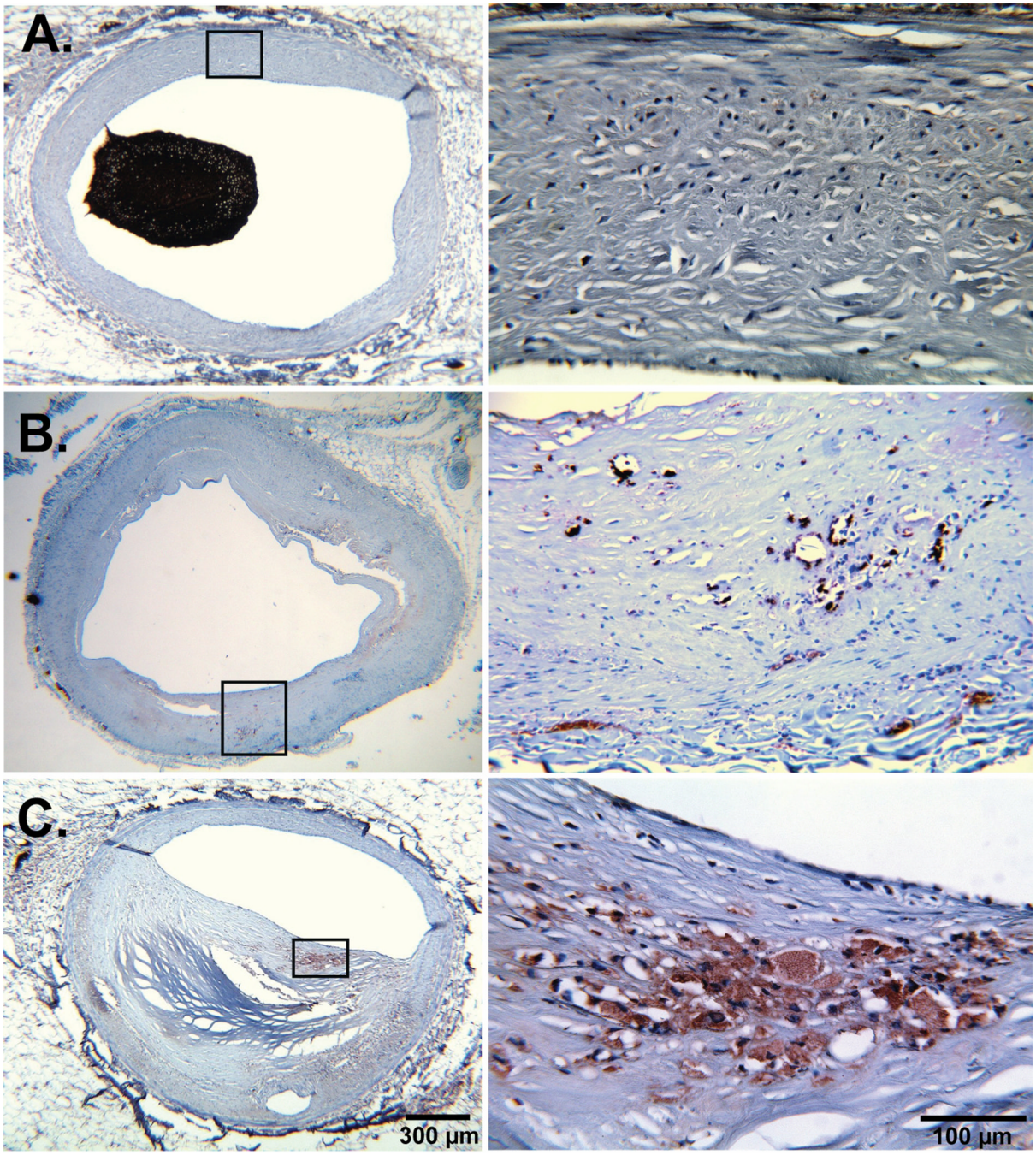

Figure 3. Glycophorin A staining in different atherosclerotic stages

Representative examples of glycophorin A staining counterstained with hematoxilin (left) of normal (A), non-stenotic (B) and stenotic plaque (C) and the corresponding magnifications (right). We did not observe evidence for erythrocyte fragments in normal coronary segments but significant positive staining in atherosclerotic plaque segments.

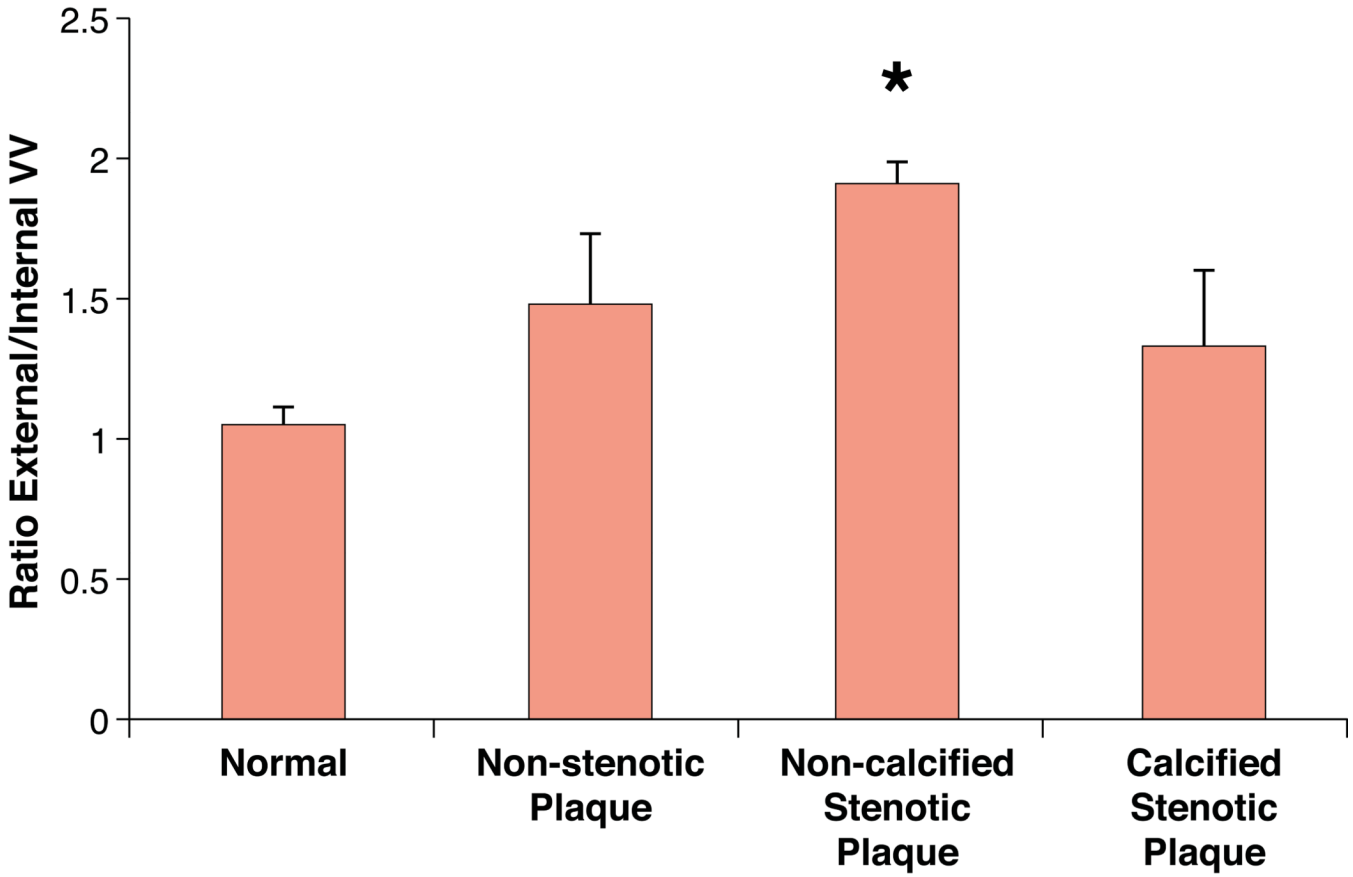

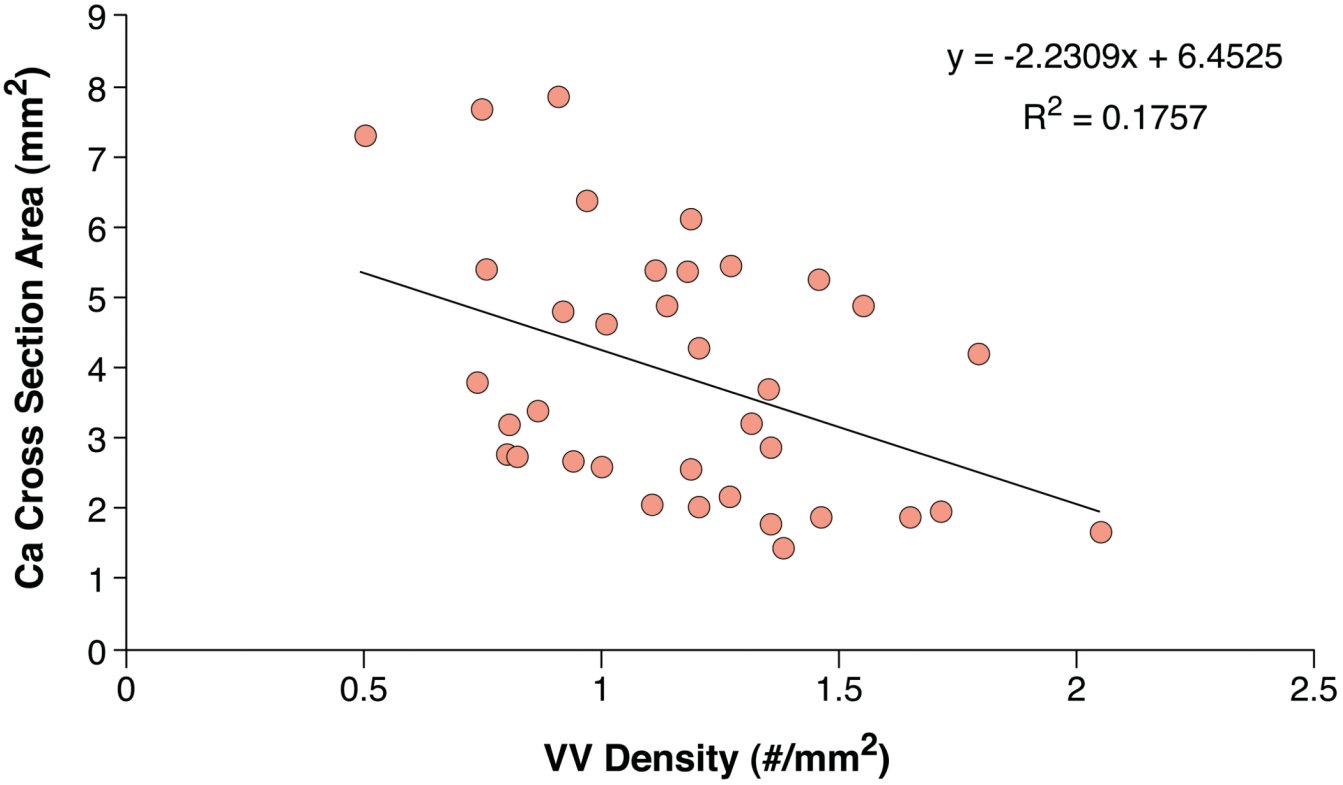

Figure 4. VV anatomy and correlation with plaque calcification area

Upper panel. This bar graph shows the ratio of external to internal VV in the four different groups. The non-calcified stenotic plaque segments showed a significant higher ratio compared to normal segments.

Lower panel. Correlation between VV density and calcium area in about four cross sections per coronary artery segment containing a calcified plaque. There was a moderate, negative correlation between VV density and calcium area in selected cross sections (r=0.42). * P<0.001

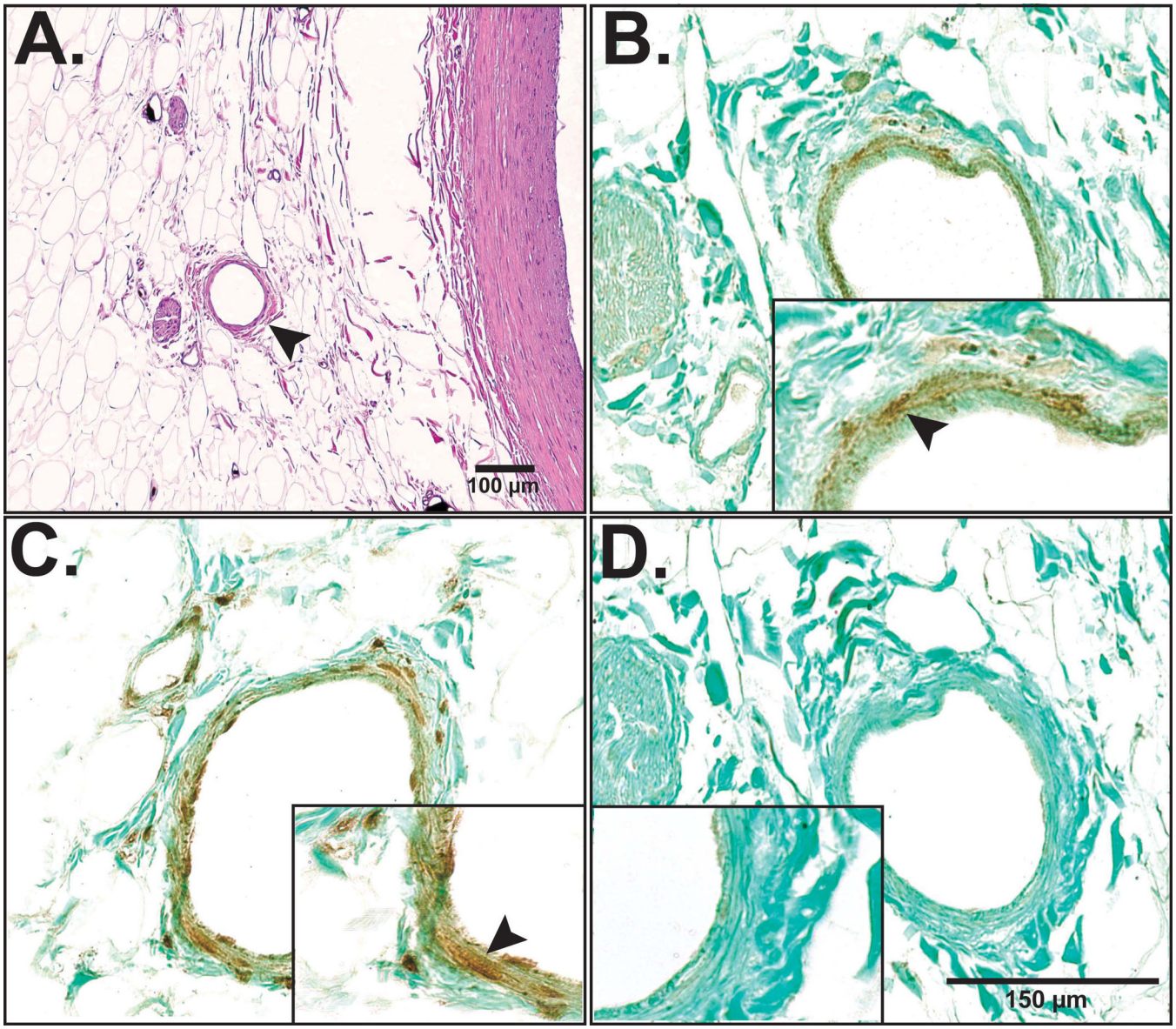

Figure 5. VV characterization with immunohistochemistry

In order to further characterize the human coronary VV (H&E stain of VV in panel A, arrow head) histology sections were stained for eNOS (panel B, arrow head), TNF-α (panel C, arrow head) and VEGF (panel D). Although eNOS and TNF-α expression were found within VV endothelial cells, VEGF expression was not detected in the current study samples.

Table 1

Patient demographics and clinical data.

n	**15**
Gender [male (%)]	10 (67)
Age [years, mean±SEM]	52±5
BMI [kg/cm^2]	24±1
Systolic Blood Pressure [mmHg]	134±9
Diastolic Blood Pressure [mmHg]	73±4
Heart rate [BPM]	79±5
Family History of Early CAD [(%)]	3 (20)
Hypercholesterolemia [(%)]	4 (27)
Hypertension [(%)]	8 (53)
Diabetes [(%)]	2 (13)
Smoking [(%)]	3 (20)

Table 2

Micro-CT and histology analysis data (mean±SEM).

	Normal (n=12)	**Non-stenotic plaque (n=18)**	**Non-calcified stenotic plaque (n=10)**	**Calcified stenotic plaque (n=10)**
Vessel wall area (mm^2/section)	5.22±0.58†	5.48±0.81†	5.63±0.62†	11.78±2.26
VV count (#/section)	4.62±0.55	12.47±1.51*	15.00±2.89#	9.22±1.30*
VV density (#/mm^2/section)	1.16±0.21	3.36±0.45$^{*,\$}$	3.72±1.03$^{*,\$}$	0.95±0.21
VV Vascular Area Fraction (mm^2/mm^2/section)	0.004±0.0006	0.01±0.001$^{\#,\$}$	0.016±0.0025$^{\#,\dagger}$	0.004±0.0007
VV Endothelial Surface Fraction (mm^2/mm^3)	0.22±0.04	0.60±0.07$^{*,\$}$	0.76±0.18$^{\#,\dagger}$	0.19±0.04
Ratio VVESA/LumenESA	0.17±0.02	0.45±0.05*	0.67±0.15$^{\#,\$}$	0.32±0.02$^{\#}$
Glycophorin A score (n=50 sections)	0.16±0.05	2.10±0.15$^{\#,\$}$	2.80±0.14$^{\#,\P,\S}$	1.58±0.15$^{\#}$
Iron score (n=50 sections)	0.10±0.04	1.88±0.15$^{\#,\$}$	2.58±0.15$^{\#,\P,\S}$	1.40±0.04$^{\#}$

Micro-CT data are normalized to the main coronary lumen radius.

*P<0.01 vs. Normal

$^{\#}$P<0.001 vs. Normal

¶P=0.001 vs. non-stenotic plaque

$^{\$}$P<0.05 vs. calcified stenotic plaque

†P<0.01 vs. calcified stenotic plaque

§P<0.001 vs. calcified stenotic plaque